Damaged Layer Characteristics in Micro-Endmilling of Copper Using an Ultrahigh-Speed Air Spindle

Jong Whan Lee
School of Mechanical Engineering, Pusan National University, San 30, Jangjeon-Dong, Geumjeong-Gu, Busan 609-735, Korea
Dong Hee Kwon
School of Mechanical Engineering, Pusan National University, San 30, Jangjeon-Dong, Geumjeong-Gu, Busan 609-735, Korea
Jeong Suk Kim*
School of Mechanical Engineering, Pusan National University, San 30, Jangjeon-Dong, Geumjeong-Gu, Busan 609-735, Korea
Duck Whan Kim
School of Mechanical Engineering, Pusan National University, San 30, Jangjeon-Dong, Geumjeong-Gu, Busan 609-735, Korea
Myung Chang Kang
National Core Research Center for Hybrid Materials Solution, Pusan National University, San 30, Jangjeon-Dong, Geumjeong-Gu, Busan 609-735, Korea
Bok Kyu Lim
Automotive Parts Innovation Center, Maegok-Dong, Buk-Gu, Ulsan 683-420, Korea

This paper presents an investigation on the characteristics of damaged layer in micro-machining by using the ultrahigh-speed air spindle. The damaged layer in metal cutting is derived from plastic deformation and transformation of metal structure. In this study, micro-cutting force, surface roughness, and plastic deformation layer according to the variation of machining conditions were investigated by experiments. The damaged layer was measured using optical microscope for the samples prepared by metallographic techniques. Its scale was dependent on cutting process parameters, especially feed per tooth. According to experimental results, it was verified that the thickness of damaged layer was increased with increasing of feed per tooth and cutting depth, also thickness of damaged layer was reduced in down-milling compared to up-milling during micro-endmilling operation.

Key Words : Damaged Layer, Micro-Endmilling, Ultrahigh-Speed Air Spindle, Copper, Micro-Cutting Force

1. Introduction

The hardness, strength and abrasion resistance of micro parts with high hardness and high precision decrease due to damaged layers in the process of machining. When such parts are used for a long time, various problems are caused due to the occurrence of residual stress. A damaged layer refers to a layer which has a nature different from that of the base metal. When a metal material is machined, such a layer is found on the surface or the outer layer in the material up to a certain

* Corresponding Author,
E-mail : juskim@pusan.ac.kr
TEL : +82-51-510-2334; **FAX** : +82-51-518-7207
School of Mechanical Engineering, Pusan National University, San 30, Jangjeon-Dong, Geumjeong-Gu, Busan 609-735, Korea. (Manuscript **Received** October 13, 2006; **Revised** December 11, 2006)

depth. The causes of damaged layers can be classified into three types : (a) damage due to contamination, absorbed layers (physical absorption and chemical absorption), chemical compound layers, mixing of foreign substances ; (b) damage due to fine crystallization layers, increase in dislocation density, generation of twins, fiber texture, abrasion transformations, transformations of crystallization owing to machining, changes in recrystallization structure textures due to frictional heat ; and (c) damage due to internal factors like residual stress layers (Matsumoto and Barash, 1984 ; Jeon et al., 2003).

A damaged layer occurring between the surface layer and the base metal in cutting is influenced by cutting speed and feed rate. In particular, in machining process in which the workpiece contacts the tool directly, damage due to the working force is notable. In this contact area, heat moves from the surface of the workpiece to the inner part. Then, a certain temperature gradient is created and damaged layers occur in this zone (Chu and Wallbank, 1998 ; Chou and Evans, 1998 ; Zhang et al., 1999).

Thus far, many studies have been conducted on damaged layers that take place on the surfaces of turning, grinding and electrical discharge machining (Chou and Evans, 1999 ; Klocke and Eisenblatter, 1997 ; Mohri et al., 1993 ; Park and Jeong, 2005).

In endmill machining, however, the likelihood of damaged layers is low due to the relatively low cutting force and cutting temperatures. Thus, there are many measuring difficulties, which hinder the progress of research. In addition, in the evaluation of machining characteristics of micro-endmilling, many studies have been carried out on macroscopic precision but the studies on microscopic precision are still very limited.

To minimize the influence of a damaged layer occurring in micro-machining, this study uses an ultrahigh-speed air spindle and performs cutting experiments with a micro carbide flat endmill. The rotation stability of the ultrahigh-speed air spindle is obtained by analyzing the vibration characteristics depending on spindle speed and selecting the stable conditions. By using a micro-machining system, the machining characteristics and surface damaged layers of copper micro-endmilling are evaluated depending on machining conditions. Besides, to acquire and analyze the cutting force of micro-machining, fine cutting force is reliably evaluated by using a newly developed tool dynamometer.

The characteristics of damaged layers is estimated by an optical microscope and this study demonstrates that the thickness of damaged layers depend on the cutting process parameters and the machining environments. Through these experiments, this study evaluates the industrial applicability of fine machining using an ultrahigh-speed air spindle is evaluated in terms of microscopic precision.

2. Dynamic Characteristics of an Ultrahigh-Speed Air Spindle

The maximum rotation frequency of the ultrahigh-speed air spindle used in this experiment is 160,000 rpm and the rotation precision of the spindle is 1 μm or less. By evaluating the characteristics of spindle air pressure, the stable conditions were selected.

As for the experiment, the rotation frequency of the spindle was measured for one minute for each of the air pressures with an optical tachometer using a jig and the measuring distance was set to be 10 mm. In consideration of measuring errors, measurement was conducted 10 times for each condition and the measurement results were averaged in order to obtain a reliable value. Through the experiment, an optimal air pressure condition (0.30~0.55 MPa) was selected for the spindle, which led to the realization of rotation stability. Fig. 1 shows the air pressure characteristics of the ultrahigh-speed air spindle.

A vibration accelerometer and an amplifier that can measure efficiently the vibration characteristics of spindle were used. In the experiment, tendencies for each condition were identified from the acceleration signals depending on spindle speeds. Fig. 2 indicates the vibration characteristics of the ultrahigh-speed air spindle. As the state of the main spindle has the dominant influence on the state of the tool, the acceleration signals were

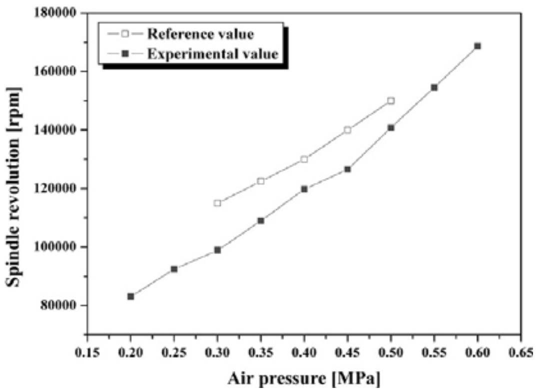

Fig. 1 Air pressure characteristics of spindle

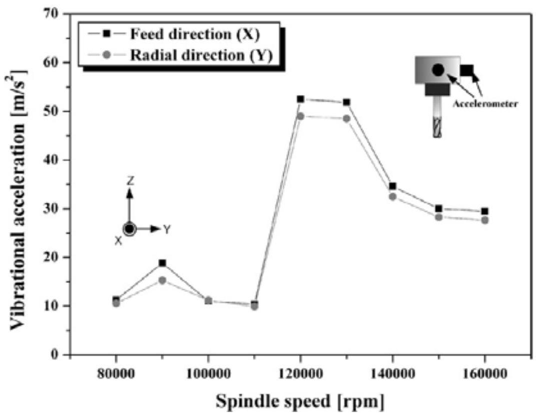

Fig. 2 Vibration characteristics according to spindle speeds

measured by attaching an accelerometer to the spindle housing in the feed direction (X axis) and the radial direction (Y axis).

The results of vibration acceleration signals depending on the spindle speeds show that the vibration acceleration values in the feed direction increase more rapidly than those in the radial direction ; in addition, the peak value can be found between 120,000 rpm and 130,000 rpm.

3. Experimental Devices and Methods

3.1 Experimental equipment and composition of devices

In this experiment, a flat-type endmill was mounted on the ultrahigh-speed air spindle and the spindle was attached to the main shaft of a high-speed

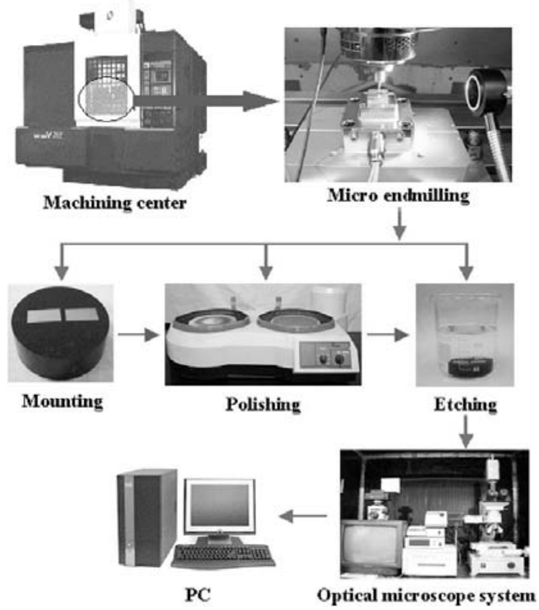

Fig. 3 Schematic diagram of experimental setup

Table 1 Specifications of experimental instruments

Instrument	Specification
Machining center	MAKINO V55 Max : 20,000 rpm, 50 m/min
Air spindle	160,000 rpm (0.6 MPa)
Micro-endmill	2-flutes flat endmill, ∅800 μm (TiAlN-coated tool)
CCD camera	Neocom (x1~450)/ PULNIX (x150)
Optical microscope system	STM-MJS2 [OLYMPUS]
Surface tester	Taylor Hobson, Surtronic 3+
Workpiece	Cu (Copper)

machining center (MAKINO V55) for machining experiment. To estimate the thickness of damaged layer, the layer was observed visibly using an optical microscope system. For measurement of the cutting force, the system was constructed to measure the micro cutting force by clamping the workpiece to an exclusive jig.

Figure 3 shows the composition of the overall experiment device diagram and Table 1 indicates the equipment and specifications used in the experiment.

Table 2 Machining conditions of experiment

	Spindle speed [rpm]	60,000～160,000 (Step : 20,000)
Copper (Cu)	Feed per tooth [μm/tooth]	3, 4, 5, 6
	Cutting depth [μm]	50, 100, 150, 200
	Cutting fluid	Dry cutting

3.2 Micro-machining experiment method

A copper material was manufactured in the form of a block to identify the characteristics of damaged layer depending on micro-endmilling conditions. For the machining experiment, fine machining condition is selected with a ∅0.8 mm micro tool at a speed of 150 m/min or above. That is, the spindle speed is set at 60,000～160,000 rpm with an increase of 20,000 rpm each time and machining was conducted depending on feed per tooth. The thickness of the damaged layer and the burr were measured through an optical microscope. For the characteristic experiment of the damaged layer, the samples were machined by 10 passes depending on the machining conditions and the machined face of the samples was measured. Table 2 shows the machining conditions applied to the micro-endmilling experiment.

When resin selection is not made properly in sample mounting, it becomes difficult to observe the edge part in the compression and rounding phenomena of the resin following mounting. Therefore, the machining process was performed by selecting the epomet resin which has a high abortion force and a high level of hardness for the samples. As for etching, natal was adjusted at 6～9% depending on the material characteristics and corrosion was made to take place for about 10 seconds. Then the thickness of damaged layer was measured by the visual differences of textures.

4. Characteristics of Damaged Layers

4.1 Shapes and sizes of damaged layers

To examine the correlations between the mechanical and thermal influences and microscopic

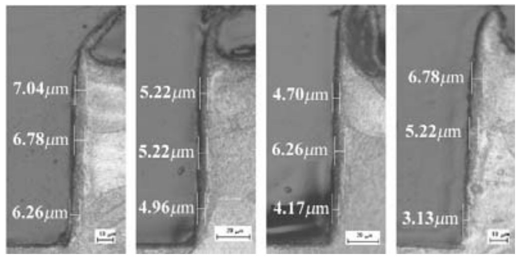

(a) Spindle speed : 60,000 rpm, Cutting depth : 100 μm, Feed per tooth : 3, 4, 5, 6 μm/tooth

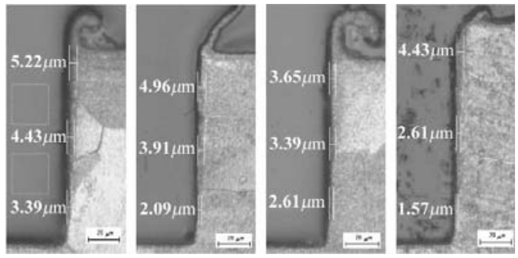

(b) Spindle speed : 120,000 rpm, Cutting depth : 100 μm, Feed per tooth : 3, 4, 5, 6 μm/tooth

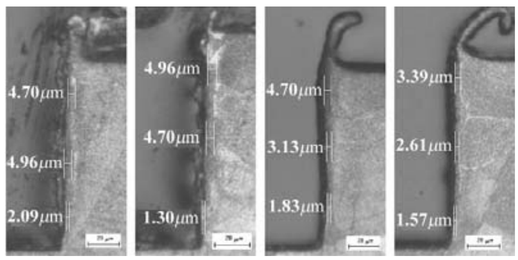

(c) Spindle speed : 160,000 rpm, Cutting depth : 100 μm, Feed per tooth : 3, 4, 5, 6 μm/tooth

Fig. 4 Thickness variation of damaged layer according to machining conditions (up-milling)

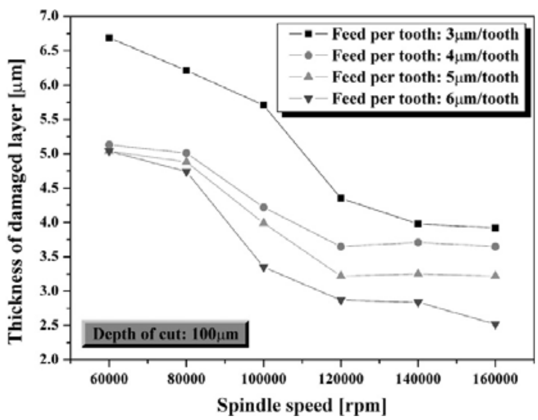

Fig. 5 Relationship between thickness of damaged layer and spindle speed (up-milling)

precision in ultrahigh-speed micro-endmilling the shape and thickness of damaged layers depending on spindle speed and feed per tooth were evaluated in terms of up-milling (upward cutting) and down-milling (downward cutting). In addition, the damaged layer of the sample was measured by the corrosion method through an optical microscope. Measurement was conducted for the upper, middle and lower parts of the damaged layers occurring on each lateral face and the average value was obtained. Figs. 4 and 5 show the shape and the thickness of damaged layers depending on feed per tooth in up-milling, while Figs. 6 and 7 indicate those depending on feed per tooth in down-milling.

The thickness of damaged layer was smaller in the down-milling of Fig. 7 than in the up-milling of Fig. 5. This can be attributed to the fact that down-milling receives less specific cutting resistance and compressive residual stress than up-milling. In Figs. 4 and 6, as the damaged layer became thicker, burrs increased consistently. As to the machined side shape of micro-endmilling, the upper part was wide and the lower part was narrow. As shown Figs. 4 and 6, burrs increased due to the runout errors on the upper machined face; and there was an increase in damaged layers. Therefore, to ensure stable machining and improve machining quality, it is necessary to minimize the tool runout.

The thickness of damaged layer showed a tendency to decrease in both up-milling and down-milling, as the spindle speed is increased. This characteristic of damaged layer can be explained by the decreased specific cutting resistance in case of high-speed cutting. As the feed per tooth increased, the thickness of damaged layers decreased in both case. This can be also attributed to the phenomenon in which the specific cutting resistance decreases in small-scale cutting when the feed per tooth increases.

4.2 Characteristics of cutting force

In micro-machining using an ultrahigh-speed air spindle, cutting force signals of very high frequency are generated due to the high spindle speed. Such signals cannot be acquired by an existing

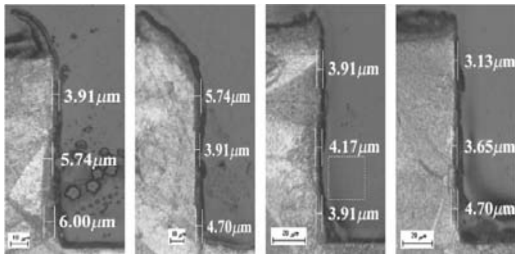

(a) Spindle speed : 60,000 rpm, Cutting depth : 100 μm, Feed per tooth : 3, 4, 5, 6 μm/tooth

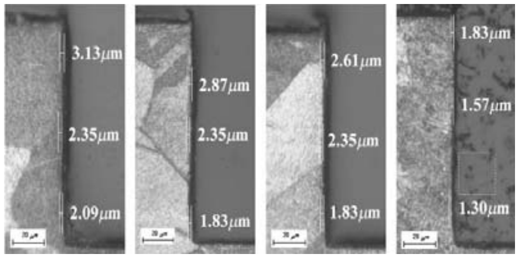

(b) Spindle speed : 120,000 rpm, Cutting depth : 100 μm, Feed per tooth : 3, 4, 5, 6 μm/tooth

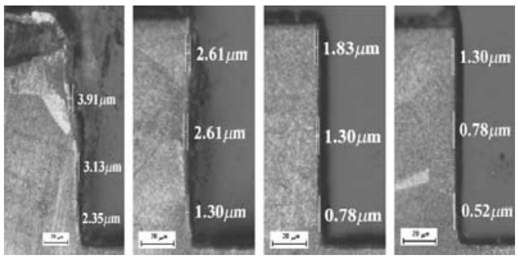

(c) Spindle speed : 160,000 rpm, Cutting depth : 100 μm, Feed per tooth : 3, 4, 5, 6 μm/tooth

Fig. 6 Thickness variation of damaged layer according to machining conditions (down-milling)

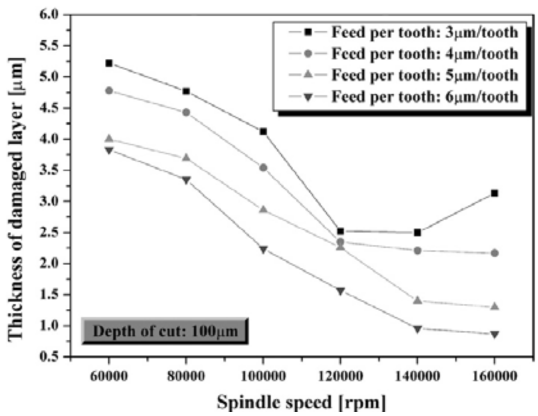

Fig. 7 Relationship between thickness of damaged layer and spindle speed (down-milling)

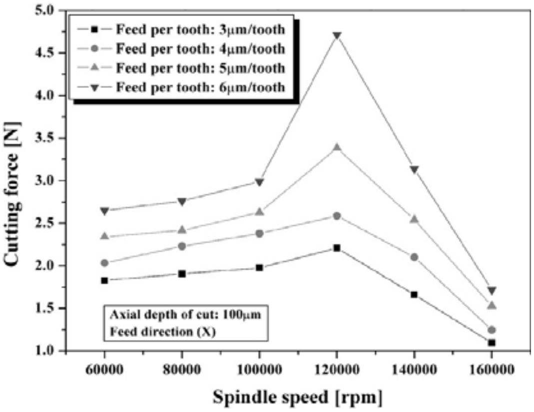

Fig. 8 Relationship between cutting force and spindle speed (feed direction)

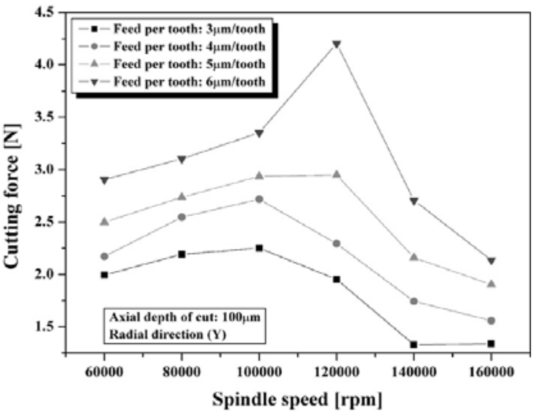

Fig. 9 Relationship between cutting force and spindle speed (radial direction)

tool dynamometer of low natural frequency and therefore it is necessary to develop a new tool dynamometer suitable for such signals. To meet such a need, a new tool dynamometer with higher response frequency was developed and applied to actual micro-machining.

In this experiment, the maximum rotation of 160,000 rpm is 5.3 kHz under the condition of using a two-teeth flat endmill. So, to measure a cutting force in stable frequency range a tool dynamometer with a resonance frequency of 10 kHz is introduced. Figs. 8 and 9 show the characteristics of cutting forces in the feed and radial directions by using this dynamometer. It is found that the cutting force characteristics depending on spindle speed are closely related to the dynamic

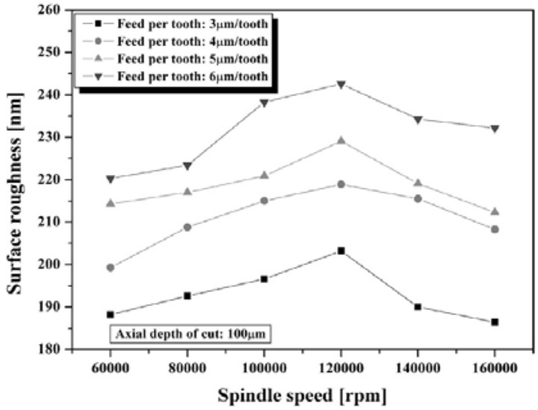

Fig. 10 Relationship between surface roughness and spindle speed

characteristics of the spindle in Fig. 2. Therefore, the occurrence of a damaged layer is not closely related to the dynamic characteristics of spindle and cutting force.

4.3 Characteristics of surface roughness

The roughness of the machined surface was measured using a Taylor Hobson three-dimensional surface roughness tester. The machined surface of the groove was measured three times and the average value was indicated in the average roughness of the central line. Fig. 10 shows the surface roughness of machined surface. The characteristics of the surface roughness are similar to that of the cutting force in the feed direction and their correlations. In macro-machining experiments, the surface roughness is often correlated with the damaged layers (Ahn et al., 2005 ; Kwon and Hong, 2005). In this micro-machining of copper, the correlation between surface roughness in Fig. 10 and damaged layers in Fig. 7 was not found.

5. Conclusions

In micro-endmilling of copper using an ultra-high-speed air spindle, the evaluation experiments of the damaged layers led to the following conclusions :

(1) Damaged layers and burrs are strongly correlated and the occurrences of damaged layers are

less frequent in down-milling than up-milling.

(2) As the spindle speed is increased, damaged layers decreased in both up-milling and down-milling and it decreased as the feed per tooth increased under the same conditions.

(3) Damaged layers occurred more frequently in the upper side surface than in the lower side surface and this seems to be caused by the constraint of the tool and runout errors.

(4) The thickness of damaged layers are not correlated with the dynamic characteristics of spindle and surface roughness of machined surface.

References

Ahn, D. K., Kim, H. C. and Lee, S. H., 2005, "Determination of Fabrication Direction to Minimize Post-machining in FDM by Prediction of Non-linear Roughness Characteristics," *Journal of Mechanical Science and Technology*, Vol. 19, No. 1, pp. 144～155.

Chou, Y. K. and Evans, C. J., 1998, "Process Effects on White Layer Formation in Hard Turning," *Transactions of NAMRI/SME*, Vol. 26, pp. 177～122.

Chou, Y. K. and Evans, C. J., 1999, "White Layers and Thermal Modeling of Hard Turned Surfaces," *International Journal of Machine Tools & Manufacture*, Vol. 39, pp. 1863～1881.

Chu, T. H. and Wallbank, J., 1998, "Determination of the Temperature of a Machined Surface," *Journal of Manufacturing Science and Engineering ASME*, Vol. 120, pp. 259～263.

Jeon, S. K., Shin, Y. J., Kim, B. H., Kim, H. Y. and Jeon B. H., 2003, "Micro-Machining of Glasses using Chemical-Assisted Ultrasonic Machining," *Transactions of KSME*, Vol. 27, No. 12, pp. 2085～2091.

Klocke, F. and Eisenblatter, G., 1997, "Dry Cutting," *Keynotepaper, Annals of CIRP*, Vol. 46, No. 2, pp. 519～526.

Kwon, W. T. and Hong, I. J., 2005, "Estimation of the Cutting Torque Without a Speed Sensor During CNC Turning," *Journal of Mechanical Science and Technology*, Vol. 19, No. 12, pp. 2205～2212.

Matsumoto, Y. and Barash, M. M., 1984, "Residual Stress in the Machined Surface of Hardened Steel High Speed Machining," *Presented at the Winter Annual Meeting of the ASME*, pp. 193～204.

Mohri, N., Saito, N. and Tsunekawa, Y., 1993, "Metal Surface Modification by Electrical Discharge Machining with Composite Electrode," *Annals of the CIRP*, Vol. 42, pp. 219～222.

Park, J. and Jeong, H., 2005, "A Study on the Fabrication of Micro Groove on Si Wafer using Chemical Mechanical Machining," *Journal of Mechanical Science and Technology*, Vol. 19, No. 11, pp. 2096～2104.

Zhang, Q. H., Zhang, J. H., Jia, Z. X. and Sun, J. L., 1999, "Material Removal Rate Analysis in the Ultrasonic Machining of Engineering Ceramics," *Journal of Materials Processing Technology*, Vol. 88, pp. 180～184.